

Layered native defects in chemically disordered topological insulators

Jakub Šebesta^{1,*} and Karel Carva¹

¹*Charles University, Faculty of Mathematics and Physics,
Department of Condensed Matter Physics, Ke Karlovu 5 121 16 Praha 2, Czech Republic
(Dated: May 28, 2022)*

Topological insulators host on their surface unique conductive electron states, characterized by their almost linear dispersion. Their properties are robust against wide range of perturbations while they respect symmetries, which leads to forming of surface states. There exist possibilities to open the surface gap by breaking the time reversal symmetry, *e.g.* by magnetic doping, which brings new possibilities for applications. In reality, however, several kinds of native defects are present in the material which influence the actual properties of the material. In the present work we focus on the presence of stacking faults, actually twinning planes, in the Bi₂Se₃ layered structures based on the TB-LMTO-ASA calculations. Their behavior under the presence of magnetic and non-magnetic chemical disorder is studied as well. Finally, the influence of the presence of twinning planes on the surface states in topological insulators is examined. We show the distribution of the twinning planes in the material in an ideal structure same as in dependence on the (non)-magnetic doping, likewise the influence on the surface gap.

Keywords: topological insulators; magnetic doping; native defects; ab-initio

I. INTRODUCTION

Topological insulators (TI) protected by time reversal symmetry (TRS) were ones of the first discovered three dimensional topological material [1–4]. Although the bulk band structure stays gaped the surface of such materials hosts unique conductive states possessing linear dispersion, which intersect in the so-called Dirac point [1, 4–7]. Forming of surface electron states comes from the occurrence of a strong spin orbit coupling (SOC), which is given by heavier elements, and the presence of TRS. It ensures band crossing in high symmetry points of the Brillouin zone, because any crystal symmetry is required (compare *e.g.* topological crystal insulators [1, 5]). Combination of strong SOC and TRS lead to the spin polarization of surface bands [3, 5, 8]. Electrons moving in the proximity of the Dirac cone with a opposite momentum have also opposite spins as well, so-called spin-momentum locking. It ensures *e.g.* a suppression of back-scattering and related great surface transport properties [9, 10].

For real applications the influence of defects could be important, since they might significantly alter properties of the ideal matter. It could be varied intentionally by chemical doping. In the case of TI, the magnetic doping is significant. It leads to breaking of TRS and therefore it opens surface gap [11, 12]. Then not only does a possible control of surface conductivity appear due to increased surface scattering, but also it could bring the occurrence of new unique phenomena as QAHE [13]. Besides, native defects occur there. Their presence is hardly controllable and they might have a significant impact of physical properties [14, 15] as well. There could exist several kinds of native defects depending on the actual compound and

the growing process. It includes also twinning planes, a kind of the plane defect we are focusing on in this article.

An important group of 3D topological insulator are bismuth chalcogenides, such as Bi₂Se₃ studied in this paper [16, 17]. This compound posses relatively simple band structure, convenient for experimental and theoretical studies, with Dirac cones at the Γ point. The crystal structure of Bi₂Se₃, belonging to the $R\bar{3}m$ space group, consists of Bi and Se hexagonal layers. They are gathered into quintuple layers (QLs), in which Bi and Se layers alter (Fig. 1). Due to coupling of QLs only by vander Waals (vdW) forces there appears a gap between QLs, so-called ‘van der Waals’ gap [17]. The presented crystal structure offers several sites, which could be occupied by magnetic atoms. Based on the theoretical and experimental studies the most probable position for Mn atom doping is a substitutional position, where the magnetic atoms replace Bi atoms (Mn^{Bi}) [18–20]. Naturally, there also appears native defect like Bi or Se anti-sites (Bi^{Se} resp. Se^{Bi}), where Bi atoms replace Se ones and *vice versa*. Theoretical studies revealed that the most favorable intrinsic defect are the Se vacancies (Vac^{Se}) [18, 21–23].

Not only point defect appears there, but also layer defects were experimentally reported. As stated in the beginning we are focusing on twinning planes (TP) are [24–26]. TP consist in stacking fault in the layered structure of bismuth chalcogenides. In their ideal structure three positionings of hexagonal layers alternate similar to close packed FCC like structures. During the growth process there exist two distinct sites, which the atoms in the new layer can occupy. Therefore mirrored stacking might arise, which could be represented by 60° rotation of new layers in relation to the ideals ones [26]. Possibly there exist a few positions where TP could appear, but the most probable one lies in the vdW gap [27]. It consists in the mirroring of the stacking of the adjacent QLs. The reported experiments showed that the presence

* Corresponding author: sebesta.j@email.cz

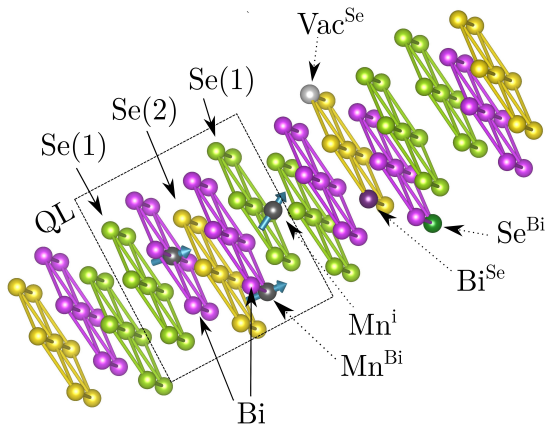


FIG. 1: Layered crystal structure of Bi_2Se_3 . Se and Bi layers gathered into QLs are depicted. Examples of (non)-magnetic defects are shown: (Mn^{Bi}) substitutional Mn atoms, (Mn^{i}) interstitial Mn atoms, (Bi^{Se}) resp. (Se^{Bi}) Bi and Se anti-sites, (Vac^{Se}) Se vacancies.

of TPs strongly depends on the used substrate [28, 29]. For clarity in the following text we will describe the position of TP by sub- and superscript denoting adjacent QLs. The notation \mathcal{T}_{x+1}^x is used for simplicity and QLs are enumerated from the vacuum interface.

Similarly to point defects, TPs might have a significant influence on the physical properties. Therefore in this paper we focus on the influence of the TP on 3D TI Bi_2Se_3 . Primarily we describe a distribution of TPs in a layer material. Then compare behavior of magnetic and non-magnetic sample. Finally, the influence of TPs on the surface states is discussed.

II. FORMALISM

The study is based on ab-initio calculations done within TB-LMTO-ASA by using the tight-binding linear muffin-tin orbital method with the atomic sphere approximation formulated in terms of Green's functions [30, 31]. It involves the local spin density approximation with Vosko-Wilk-Nursain exchange potential and using of a s, p, d atomic model [32]. Calculations were treated in the scalar relativistic approximation, where on-site spin-orbit coupling was involved into the scalar relativistic Hamiltonian as a perturbation. A basic screened impurity model was included to improve treating electrostatics of disordered systems [33]. Thanks to using of Green's function formalism a chemical disorder could be treated within the coherent potential approximation (CPA) [34]. It allows to avoid using of large statistical ensembles and it is suitable for small perturbation in the system. To simulate a layered structure, which is important to treat TPs, layered Green's functions reflecting translation symmetry only in a layer were involved [31]. The multilayer sys-

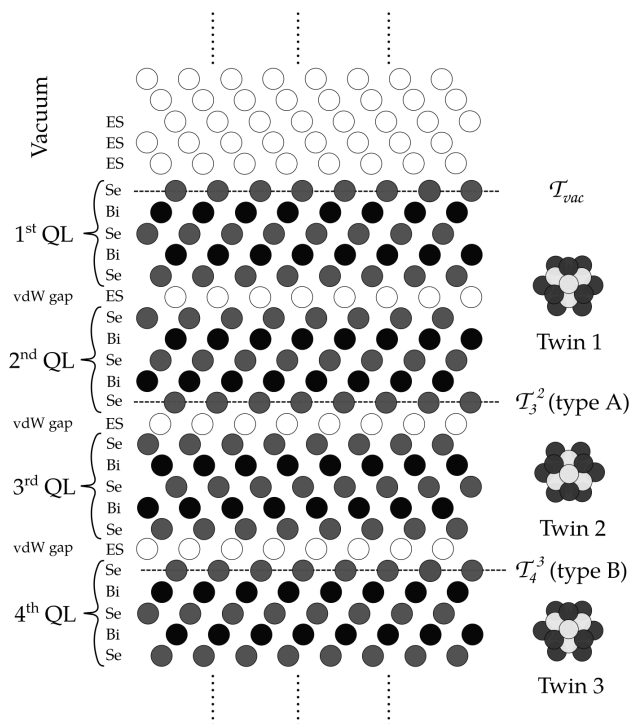


FIG. 2: Layout of the simulated multilayer Bi_2Se_3 structure including twinning planes. Proportions of atoms are neglected.

tem was attached to the semi-infinite leads, which have to satisfy self-consistent conditions. Thanks to the coupling of multilayer to the attached lead it is possible to obtain self-consistent solution also for the inner layers.

The crystal structure was based on the experimental lattice parameters (Bi_2Se_3 unit cell $a = 4.138 \text{ \AA}$ and $c = 28.64 \text{ \AA}$ [17]), which were used to build the multilayer structures. The vdW gap in between QLs was included in ASA by placing empty spheres (ES). In a similar sense the vacuum above the multilayer was included as it was formed from the fcc-like stacked empty sphere layers keeping the three-fold symmetry of Bi_2Se_3 layers. Because leads should fit to the simulated structure scandium was selected. Its hcp crystal structure suits to fcc like stacking within QLs and it possesses not too much distinct lattice parameters [35]. The multilayer consists on intermediate Sc layers of the borders, then ten or twenty QLs and ten layers of ESs, which is a sufficient number to simulate the vacuum and to obtain surface gapless states. The vdW gap involving in QLs was kept in the interface between Bi_2Se_3 and the bottom (bulk) lead, including the intermediate layers. Native defects (Bi^{Se}) same as magnetic Mn^{Bi} doping were treated. In general, mentioned defect occupied the appropriate sites with the same probability, unless otherwise stated. The influence of the defects on the crystal structure was reflected by local lattice relaxation similar to previous bulk calculation of Bi_2Te_3 and Bi_2Se_3 [14]. The relaxation cor-

responding to the presence of surfaces is not included in our calculations. In our calculation we simulate TPs in the vdW gaps with respect to the required 2D periodicity in the layer. Hence no structure boundaries within a layer, which are related to the presence of TP [24], were involved.

III. RESULT AND DISCUSSION

Initially the formation energy of TPs and its distribution in pure layered materials was studied. We compare total energies of structures without a TP with total energies of structures including various positioning of TPs within Bi_2Se_3 to obtain the formation energy of TPs. Simulations include likewise distinct stacking at the Bi_2Se_3 multilayer boundaries and different numbers of TPs.

In the simulated structure possessing the vacuum and bulk interface a TP can be placed in two different ways. It has to lie at a Se layer neighbouring to the vdW gap. Since, a TP can appear either on the vacuum or the bulk side of vdW gap. We denote it as type A resp. type B (Fig. 2). Calculated formation energies revealed a significant difference between mentioned types of TPs. Obtained negative values of the formation energy belonging to the presence of the A-typed TPs favour its occurrence in the simulated ideal Bi_2Se_3 multilayer structure, regardless of the position of TPs (Fig. 3). Whereas relatively high positive formation energies belong to B-typed TPs. We verified the influence of the surrounding on the obtained results using stacking exceptions in the initial ABC stacking. We introduced TPs at the vacuum and bulk interface (\mathcal{T}_{vac} and \mathcal{T}_{sub}) same as stacking faults (\mathcal{F}_{vac} resp. \mathcal{F}_{sub}) consisting in changes of ABC liked stacking in the vicinity of the interface. We observed only a relatively small impact on the formation energies, which depends on the distribution of TPs (Fig. 3)

The calculations for a single TP in a 10 QL width multilayer show a tendency of TPs to incline toward the bulk interface regardless of the stacking at the interfaces (Fig. 3). In the vicinity of Bi_2Se_3 boundaries the calculated energy curves split according to the stacking at the interface. The shown splitting in the proximity of the vacuum interface is manifestation of using the ASA in our calculations. The form of the spacer simulating the vacuum (Fig. 2), which consists of layers of empty spheres, influence naturally physical properties. Presence of \mathcal{T}_{vac} keeps the results roughly intact. Only the formation energy for TPs close to the interface become more negative. The effect is the more pronounced the more serious perturbation appears (\mathcal{F}_{vac}). The observed changes of the formation energy are given by the interaction of the studied TPs in the multilayer with perturbed stacking of vacuum layers. It arises from the change of the stacking order of ESs in the vicinity of the surface and their tiny non-zero charge density, which spreads from the surface layer. Similarly an opposite effect is indi-

cated at the bulk side in dependence on the structure of the substrate. A different magnitude of the effect comes from a different structure of \mathcal{F}_{vac} and \mathcal{F}_{sub} . The location of the perturbation is important as well. It can be depicted by a distribution of charge transfer $\Delta\rho_t$ through the structure (Fig. 4). It describes the change of the distribution of atomic charges caused by a TP. We observed that the charge perturbation in the case of the A-typed TPs spreads from the mirror layer mainly towards the vacuum interface and *vice versa* for the B type. It corresponds to the shape of calculated energy dependencies (Fig. 3). They evince a tendency to the elongation of the region possessing the majority of the perturbation. One can assume the influence of the electrostatic interaction related to a TP and interfaces. The interaction with the interface is likely responsible for the different sign of the formation energy obtained by our calculations. The influence of the interfaces is clearly depicted by the asymmetry in Fig. 4. They have significant impact on the vicinity of TP in the otherwise symmetrical structure (Fig. 2). Hence one can assume that the dominating interaction with the substrate suppresses B-typed TPs. Whereas the loose vacuum interface allows relaxation of the system perturbed by A-typed TPs.

The obtained negative values of the formation energy belonging A-typed TPs correspond to the experimental observation of TPd in real undoped samples [24–26]. Then a tendency to form stacking faults related to the negative formation energy seems to be a natural form of decreasing total energy of the ideal structure. The observed difference in the formation energies between TPs in surface and bulk layers might lead to a distinct behavior during annealing. Hence the probability of forming TP [24] should be higher in the bulk then in the surface and *vice versa*. Based on the structural measurements one could also conclude that there is no twin defect close to the surface. Usually TPs are distant more than 10 QLs from the surface [26]. Less stability of TPs in the vicinity of the sample surface indicates, that it might be easy to get rid of it by annealing of the sample. We note that a general dependence of the formation energy on the density of such stacking faults is out of the scope of this article. Further, in the following text we deal only with A-typed TPs unless otherwise stated.

The presented calculations showed an interplay between close stacking faults. One can observe it in the mentioned splitting of energy dependencies, where it is represented by an extra energy contribution (Fig. 3). The interaction between TPs was studied by introducing an extra TP in the structure (Fig. 5). The position of one TP was kept fixed there while the another was approached to it. We found that the initial dependence obtained for a single TP (Fig. 3) is changed only for the adjacent TPs, where appears an extra interaction energy (Fig. 5). Because of the strong effect given by interfaces, we introduces a larger system with two fixed TP and the third one moving in between (Fig. 6). It helps us to get rid of the effects caused by the inter-

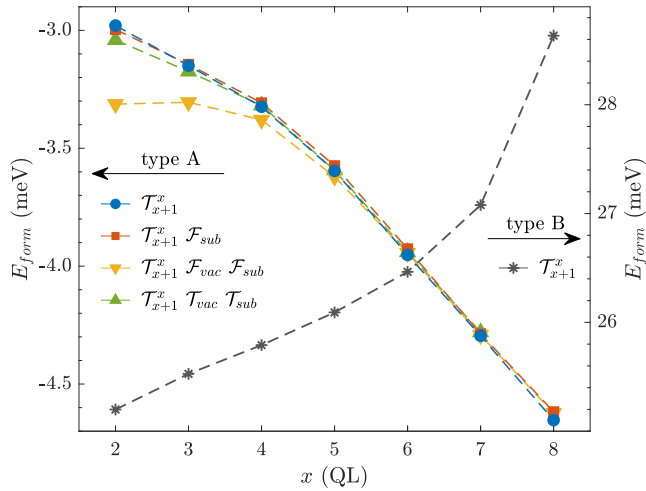


FIG. 3: Dependence of the formation energy E_{form} on the position of TP x in the Bi_2Se_3 multilayer. Dependencies for two different types of TPs are depicted. It includes various stacking at the interfaces as well. \mathcal{T}_{vac} and \mathcal{T}_{sub} denotes TP at the vacuum resp. bulk interface. Similarly $\mathcal{F}_{vac/sub}$ denotes stacking fault of the surrounding in the vicinity of interfaces. Bi_2Se_3 multilayer consists of 10 QLs.

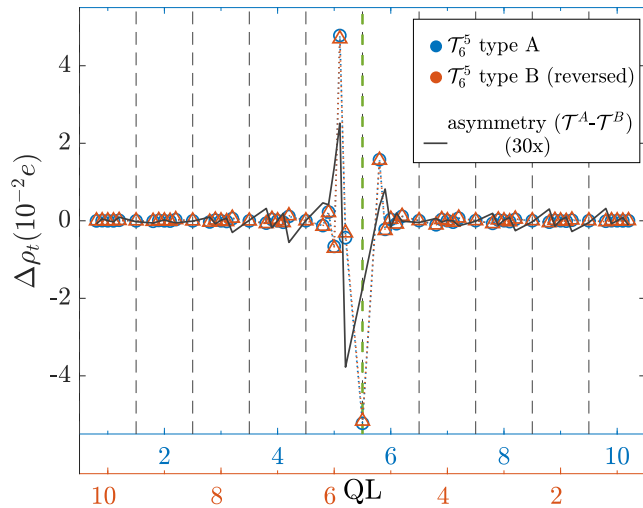


FIG. 4: Dependence of the charge transfer $\Delta\rho_t$ on the position and the type of TPs. Charge transfer represents the change of the charge distribution in a structure with a TP in relation to the unperturbed one.

faces, which are presented *e.g.* in bending or in splitting of calculated curves (Figs. 3, 5). The new approach gives a similar behavior to the previous one (Fig. 5), but with a clearly visible repulsion energy of the neighboring TPs (Fig. 6a). Whereas for distances over two QLs no effect was observed. It showed that TPs in a pure sample are likely spread over the sample with distances at least of the width of three QLs. Experiments prove that if more than one twin plane is observed, they are clearly

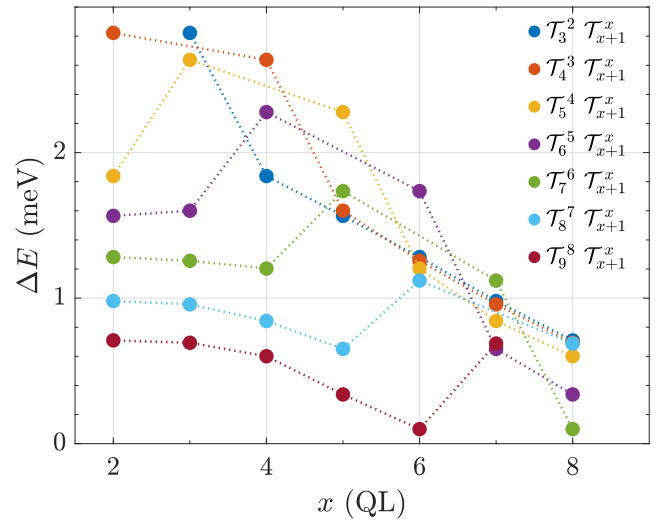


FIG. 5: Dependence of the relative formation energy (ΔE) on the position of TP x in the Bi_2Se_3 layer. Energy dependencies for systems with two TPs within the Bi_2Se_3 multilayer, which consists of 10 QLs, are depicted.

several 10nm apart [26]. One should be aware that we are comparing ground state calculations with a molecular beam epitaxy growth, which occurs far from equilibrium conditions.

The described behavior dramatically changed when a chemical disorder is introduced in the sample. Regardless of the type of doping, whether is magnetic (Mn^{Bi} , Fig. 6b) or not (Se^{Bi} , Fig. 6c), we observed a modification of distributions of TPs in comparison to the pure sample (Fig. 6a). Calculations showed that a magnetic disordered (Mn^{Bi}) leads to gathering of TPs instead of their spreading, which was observed in the undoped system. Whereas non-magnetic disorder almost removes presence of any preferred positions as no significant energy difference was observed (Fig. 6c) in comparison to the ideal one (Fig. 6a). The energy differences are about one order of magnitude smaller in the case of non-magnetic doping.

We assume that gathered TPs in the case of magnetic doping likely minimize the induced effect on the electron structure. It is caused by interplay of TPs and disorder in connection with the magnetism, which naturally doesn't exist in the pure structure. It likely indicates that TPs are not too favorable in the magnetically disordered systems as the dependence of the relative formation energy on the defect concentration proves (Fig. 7).

The flatten dependencies calculated for the non-magnetic disorder likely originates from the suppressed influence of TPs on Bi_2Se_3 multilayer under the presence of a chemical disorder in comparison to the ideal case. Therefore it emphasises the importance of the magnetism in the interplay with presented TPs in the case of magnetic doping. A general disorder represents only a small contribution. We can assume that the strong modifica-

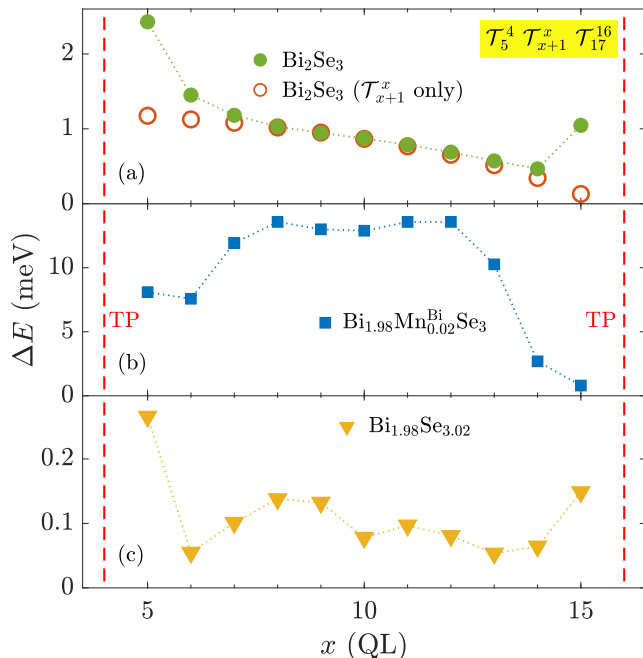


FIG. 6: Relative formation energy (ΔE) in dependence on the position x of the middle TP in the system with fixed border TPs. The Bi_2Se_3 multilayer consist of 20 QLs. Comparison of pure and (non-) magnetically disordered systems is depicted. Unfilled points in the plot (a) denoted the structure without border TPs.

tion of the energy dependencies (Figs. 6b vs. 6c) is based on the presence of the magnetism.

To describe the influence of the type of the disorder on the presence of TPs, we calculated dependencies of the formation energy on the concentration x of Mn^{Bi} or Se^{Bi} defects (Fig. 7). The calculations were done with a homogeneous doping of the sample. Results obtained for various possible stacking prove that increased amount of magnetic dopants x leads to the suppression of the TPs in the multilayers. Distinct curves for a particular defect denotes different surrounding similarly to Fig. 3. On the other hand the non-magnetic disorder (Se^{Bi}) decreases formation energy of TPs in the structure. It corresponds to the discussed suppressed impact of TPS in the case of the non-magnetic disorder.

Later we focused on the influence of TP on the behavior of magnetic Mn dopants. In comparison to the sample with unperturbed stacking we observed that the presence of a TP changes its likelihood in the QL adjacent to the TP (Fig. 8) as favored and unfavored sites appears. The relative formation energy differs for distinct substituted Bi sites within OL. There exist two Bi sites per QL (Fig. 8). The influence of TPs on the electron structure of a particular QL can be reflected *e.g.* by site-resolved magnitudes of magnetic moments. It shows significant enhancing of magnitudes of magnetic moments on the one side of the TP according to the location of the perturbation depicted by the charge transfer

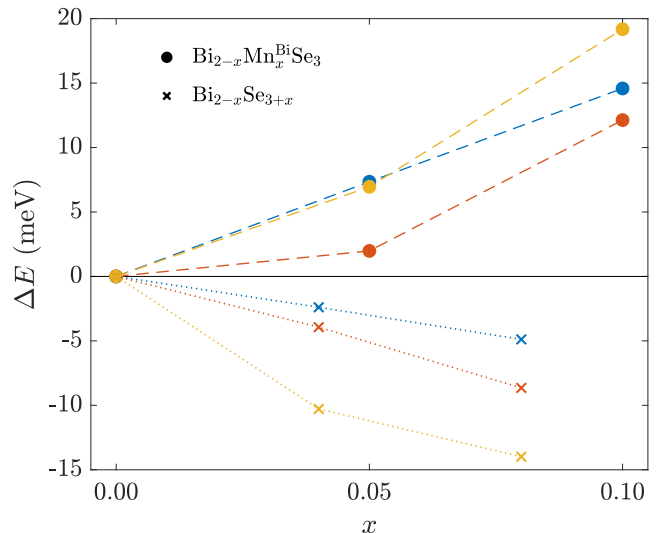


FIG. 7: Relative change of the TP formation energy in dependence on the concentration of defects. Results for several different stacking at the multilayer interface are plotted. Two TPs (\mathcal{T}_4^3 and \mathcal{T}_8^7) in Bi_2Se_3 multilayer consisting of 10 QLs were used.

(Fig 4). The variation of magnitudes of magnetic moments also corresponds to similar features observed at the boundaries, because the mirrored stacking caused by TP could behave as an extra interface. By comparison the obtained dependencies of relative formation energy with magnitudes of magnetic moments one could observe a clear correspondence between the enhanced magnetic moments and the disfavored position in the vicinity of TP and *vice versa* (Fig. 8). Described interplay of TPs and magnetic defects could explain the energetic gain observed for gathered TPs in magnetic material (Fig. 6). Close TPs lead to smaller perturbation of the whole electron structure.

The TI are studied especially due to the occurrence of the conductive Dirac surface states. The appearance of TP can strongly influence their presence since the mirroring of the structure symmetry could represent a boundary in the structure. Hence, in this paper we also try to simulate the influence of the presence of TP and its position on the surface states. We calculated Bloch spectral function (BSF) in the vicinity of the Γ point, where the Dirac cone exists, on the path between high symmetrical reciprocal points M and K . Because BSF isn't too much convenient for the comparison of the investigated structures, it was projected along k -axis to the energy axis, which result in easily handled line plots. The projected BSFs (PBSF) reveal that presence of a TP in a certain distance from the surface breaks the surface Dirac states regardless of the structure of the vacuum interface (Fig. 9). Our calculations showed that for TPs which are closer than 6 QL to the surface the surface gap become opened. The PBSF curves don't reach zero values in the suggested gap partly due to the insufficiently fine mesh in the energy axis and

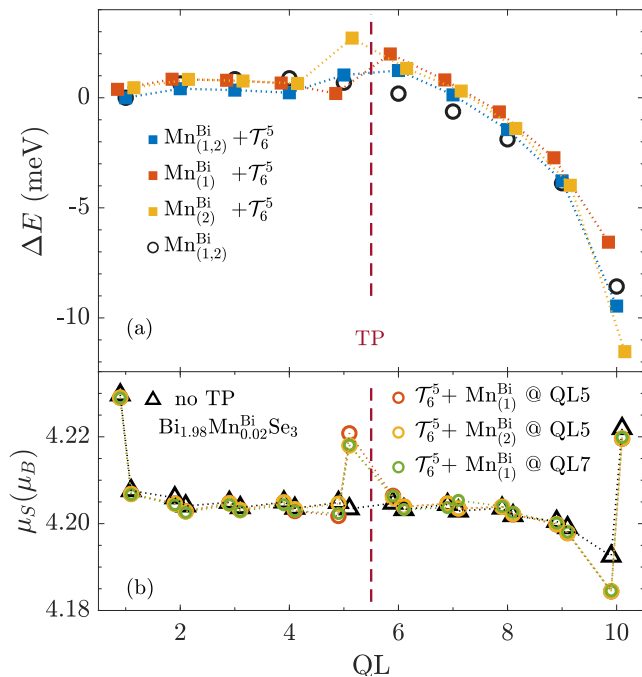


FIG. 8: Magnetically doped Bi_2Se_3 multilayer. (a) Relative formation energy in dependence on the position of magnetic doping. The index of Mn^{Bi} in the key denotes which positions in QL were doped. 1% of Bi atoms is substituted in selected QL. Circles denoted the unperturbed structure. The curve is shifted in the energy axis for better comparison. (b) Distribution of the magnitudes of effective magnetic moments: (triangles) homogeneously doped sample, (circles) selective doping. For unoccupied site the effective magnetic moment related to the zero concentration in the CPA is depicted. To each QLs position two data points are assigned due to the presence of two Mn^{Bi} sites within QL.

because of a presence of ingap states. They appear especially under presence of \mathcal{T}_4^3 (Fig. 9). Their dependence on the vacuum interface indicates a surfaces character of the states. The states likely originate from the interplay between the TP and the interface since they disappear with a distant TP.

As it was mentioned the observed canceling of surface states and gap opening likely arise from the proximity of two interfaces, which lead to a destructive interference [6]. Comparing results obtained for TP below the seventh QL with the unperturbed system we found almost no difference.

Influence of the surface gap in Mn doped $\text{Bi}_{2-x}\text{Mn}_x\text{Se}_3$ multilayers by TPs can be observed as well. We used there a homogeneous doping of substitutional Mn defect, which is the most favorable position [18, 19]. We found that initial surface gap observed for the concentration of $x = 0.1$ significantly changes in the proximity of the TP, where the surface gap become wider. The surface gap

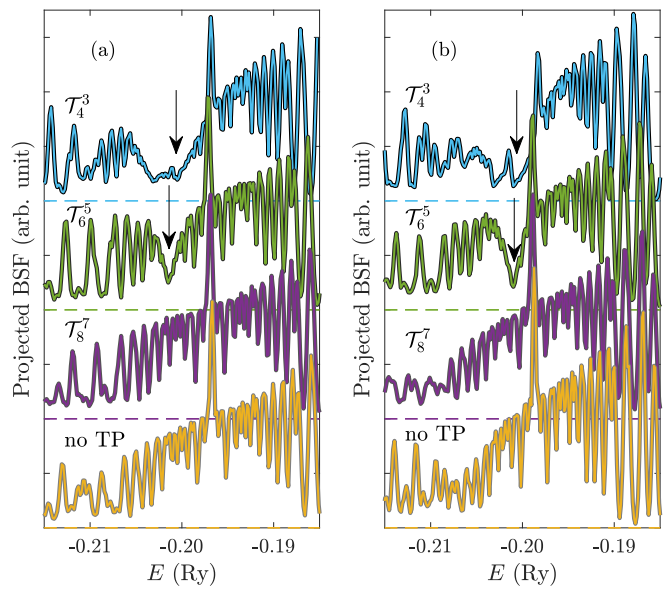


FIG. 9: Integrated BSF of surface QL in the vicinity of Γ point, pure Bi_2Se_3 . Spin up and spin down channels are overlaying. The obtained surface gap in denoted by arrows. (a) continuous stacking of ES in vacuum region, (b) ES stacking exception in the vicinity of the surface (\mathcal{F}_{vac})

width initially depends of the vacuum interface structure. The presence of \mathcal{F}_{vac} leads to about 0.3 mRy narrower energy gap. However, the influence of a TP on the gap width is almost same. The energy gap spreads similarly for both types of interfaces

Same as in the previous case the enhanced gap might be explained by the interaction of electron states appearing at the interfaces represented by the surface with the TP resembling an extra boundary. The non-negligible overlap of such boundary states leads to the opening of the surface gap as it was experimentally observed for thin samples [6]. Considering discovered distribution of TP in the multilayer structure one can suppose that TP might seriously influence the surface states especially in thin non-magnetic layers or multilayer structures composed of them.

IV. CONCLUSION

Using the layered structure calculation we studied behavior of TPs in the pure layered Bi_2Se_3 system same as under the presence of (non-)magnetic disorder. The influence of TPs on properties of Bi_2Se_3 was studied as well.

Initially the estimation of the formation energy of TPs in the pure layered system was done, which shows a tendency to form TPs in the undoped structure. Besides the influence of the type of the chemical disorder on the TP formation energy was studied. Calculations reveal a

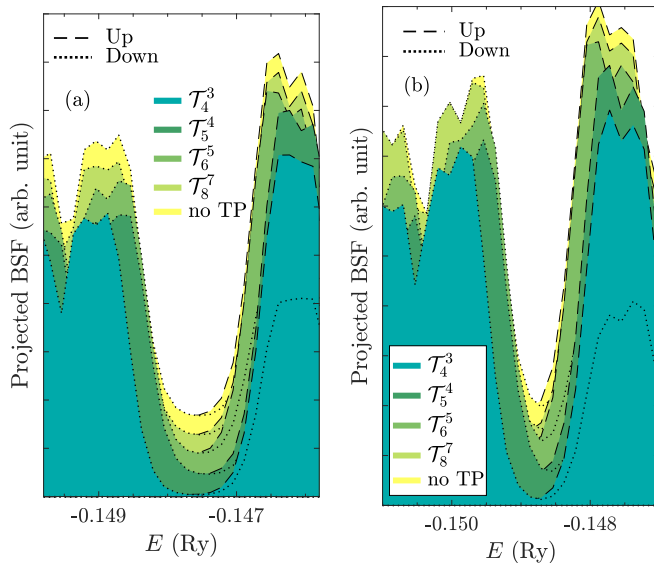


FIG. 10: Dependence of the energy width of the surface gap in the magnetically doped $\text{Bi}_{1.9}\text{Mn}_{0.1}\text{Se}_3$ multilayers. Spin channels are depicted. The origins of dependencies are shifted in the PBSF-axis for a better visibility. (a) continuous stacking of ES in vacuum region, (b) ES stacking exception in the vicinity of the surface (\mathcal{F}_{vac})

suppression of the formation of TPs in the magnetically doped structure. The comparison with the non-magnetic cases manifests the importance of magnetic interactions.

The analysis of the distribution of TPs in the pure Bi_2Se_3 indicates a higher stability of TPs in the bulk region, which correspond to the experimental results and it might be important in the case of annealing of the sample. Calculating total energies for various distributions of several TPs in the multilayer structure we describe the interaction between TPs dependent on the state of

doping. Calculation show that TPs in the pure Bi_2Se_3 almost don't influence each other in distances over tree QLs. The distribution of TPs and their interplay significantly change under presence of a chemical disorder. The presence of a non-magnetic disorder weakens the influence of TPs on the electron structure and therefore the interactions between TPs are significantly smaller. The presence of the magnetism totally transforms the stated behavior. The calculated distribution of TPs revealed that adjacent TPs are energetically favorable. Gathering of the TPs corresponds to the found positive contribution to the formation energy of TPs related to the magnetic doping. Therefore the observed gathering of TPs could be comprehended as its annihilation. The interplay of TPs and magnetic defects clearly demonstrate the appearance of energy preferred sites for magnetic defect in the vicinity of TPs.

Finally, the influence of TPs on the surface states was studied. We showed that the surface gap in the proximity of TP is opened. Similarly, the magnetic surface gap in magnetically doped samples is enlarged. Therefore, the presences of TPs might significantly impact transport properties.

ACKNOWLEDGEMENT

Access to computing and storage facilities owned by parties and projects contributing to the National Grid Infrastructure MetaCentrum provided under the programme “Projects of Large Research, Development, and Innovations Infrastructures“ (CESNET LM2015042), is greatly appreciated.

This work was supported by The Ministry of Education, Youth and Sports from the Large Infrastructures for Research, Experimental Development and Innovations project “IT4Innovations National Supercomputing Center LM2015070“.

-
- [1] A. Bansil, H. Lin, and T. Das, *Rev. Mod. Phys.* **88**, 021004 (2016).
 - [2] Y. Xia, D. Qian, D. Hsieh, L. Wray, A. Pal, H. Lin, A. Bansil, D. Grauer, Y. S. Hor, R. J. Cava, and M. Z. Hasan, *Nature Physics* **5**, 398 EP (2009).
 - [3] X.-L. Qi and S.-C. Zhang, *Rev. Mod. Phys.* **83**, 1057 (2011).
 - [4] D. Hsieh, Y. Xia, D. Qian, L. Wray, F. Meier, J. H. Dil, J. Osterwalder, L. Patthey, A. V. Fedorov, H. Lin, A. Bansil, D. Grauer, Y. S. Hor, R. J. Cava, and M. Z. Hasan, *Phys. Rev. Lett.* **103**, 146401 (2009).
 - [5] M. Z. Hasan and C. L. Kane, *Rev. Mod. Phys.* **82**, 3045 (2010).
 - [6] Y. Zhang, K. He, C.-Z. Chang, C.-L. Song, L.-L. Wang, X. Chen, J.-F. Jia, Z. Fang, X. Dai, W.-Y. Shan, S.-Q. Shen, Q. Niu, X.-L. Qi, S.-C. Zhang, X.-C. Ma, and Q.-K. Xue, *Nature Physics* **6**, 584 EP (2010).
 - [7] J. Cayssol, *Comptes Rendus Physique* **14**, 760 (2013), topological insulators / Isolants topologiques.
 - [8] B. Bernevig and T. Hughes, *Topological Insulators and Topological Superconductors* (Princeton University Press, 2013).
 - [9] M. König, S. Wiedmann, C. Brüne, A. Roth, H. Buhmann, L. W. Molenkamp, X.-L. Qi, and S.-C. Zhang, *Science* **318**, 766 (2007), <https://science.sciencemag.org/content/318/5851/-766.full.pdf>.
 - [10] F. Ortman, S. Roche, and S. Valenzuela, *Topological Insulators: Fundamentals and Perspectives* (Wiley-VCH, 2015).
 - [11] L. A. Wray, S.-Y. Xu, Y. Xia, D. Hsieh, A. V. Fedorov, Y. S. Hor, R. J. Cava, A. Bansil, H. Lin, and M. Z. Hasan, *Nature Physics* **7**, 32 EP (2010).
 - [12] S.-Y. Xu, M. Neupane, C. Liu, D. Zhang, A. Richardella, L. Andrew Wray, N. Alidoust, M. Leandersson, T. Balasubramanian, J. Sánchez-Barriga, O. Rader, G. Landolt,

- B. Slomski, J. Hugo Dil, J. Osterwalder, T.-R. Chang, H.-T. Jeng, H. Lin, A. Bansil, N. Samarth, and M. Zahid Hasan, *Nature Physics* **8**, 616 EP (2012), article.
- [13] C.-Z. Chang, J. Zhang, M. Liu, Z. Zhang, X. Feng, K. Li, L.-L. Wang, X. Chen, X. Dai, Z. Fang, X.-L. Qi, S.-C. Zhang, Y. Wang, K. He, X.-C. Ma, and Q.-K. Xue, *Advanced Materials* **25**, 1065 (2013), <https://onlinelibrary.wiley.com/doi/pdf/10.1002/adma.201203493>.
- [14] K. Carva, J. Kudrnovský, F. Máca, V. Drchal, I. Turek, P. Baláž, V. Tkáč, V. Holý, V. Sechovský, and J. Honolka, *Phys. Rev. B* **93**, 214409 (2016).
- [15] F. Mca, J. Kudrnovsk, P. Bal, V. Drchal, K. Carva, and I. Turek, *Journal of Magnetism and Magnetic Materials* **474**, 467 (2019).
- [16] H. Zhang, C.-X. Liu, X.-L. Qi, X. Dai, Z. Fang, and S.-C. Zhang, *Nature Physics* **5**, 438 EP (2009), article.
- [17] W. Zhang, R. Yu, H.-J. Zhang, X. Dai, and Z. Fang, *New Journal of Physics* **12**, 065013 (2010).
- [18] J.-M. Zhang, W. Ming, Z. Huang, G.-B. Liu, X. Kou, Y. Fan, K. L. Wang, and Y. Yao, *Phys. Rev. B* **88**, 235131 (2013).
- [19] Y. S. Hor, P. Roushan, H. Beidenkopf, J. Seo, D. Qu, J. G. Checkelsky, L. A. Wray, D. Hsieh, Y. Xia, S.-Y. Xu, D. Qian, M. Z. Hasan, N. P. Ong, A. Yazdani, and R. J. Cava, *Phys. Rev. B* **81**, 195203 (2010).
- [20] E. D. L. Rienks, S. Wimmer, P. Mandal, O. Caha, J. Rika, A. Ney, H. Steiner, V. Volobuev, H. Groiss, M. Albu, S. Khan, J. Minar, H. Ebert, G. Bauer, A. Varykhalov, J. Snchez-Barriga, O. Rader, and G. Springholz, **arXiv:1810.06238** (2018).
- [21] Y. S. Hor, A. Richardella, P. Roushan, Y. Xia, J. G. Checkelsky, A. Yazdani, M. Z. Hasan, N. P. Ong, and R. J. Cava, *Phys. Rev. B* **79**, 195208 (2009).
- [22] D. O. Scanlon, P. D. C. King, R. P. Singh, A. de la Torre, S. M. Walker, G. Balakrishnan, F. Baumberger, and C. R. A. Catlow, *Advanced Materials* **24**, 2154 (2012), <https://onlinelibrary.wiley.com/doi/pdf/10.1002/adma.201200187>.
- [23] A. Wolos, A. Drabinska, J. Borysiuk, K. Sobczak, M. Kaminska, A. Hruban, S. G. Strzelecka, A. Materna, M. Piersa, M. Romaniec, and R. Diduszko, *Journal of Magnetism and Magnetic Materials* **419**, 301 (2016).
- [24] D. L. Medlin and N. Y. C. Yang, *Journal of Electronic Materials* **41**, 1456 (2012).
- [25] Y. Lee, S. Punugupati, F. Wu, Z. Jin, J. Narayan, and J. Schwartz, *Current Opinion in Solid State and Materials Science* **18**, 279 (2014).
- [26] D. Kriegner, P. Harcuba, J. Veselý, A. Lesnik, G. Bauer, G. Springholz, and V. Holý, *Journal of Applied Crystallography* **50**, 369 (2017).
- [27] D. L. Medlin, Q. M. Ramasse, C. D. Spataru, and N. Y. C. Yang, *Journal of Applied Physics* **108**, 043517 (2010), <https://doi.org/10.1063/1.3457902>.
- [28] N. V. Tarakina, S. Schreyeck, M. Luysberg, S. Grauer, C. Schumacher, G. Karczewski, K. Brunner, C. Gould, H. Buhmann, R. E. Dunin-Borkowski, and L. W. Molenkamp, *Advanced Materials Interfaces* **1**, 1400134 (2014), <https://onlinelibrary.wiley.com/doi/pdf/10.1002/admi.201400134>.
- [29] I. Levy, T. A. Garcia, S. Shafique, and M. C. Tamargo, *Journal of Vacuum Science & Technology B* **36**, 02D107 (2018), <https://doi.org/10.1116/1.5017977>.
- [30] H. L. Skriver, *The LMTO Method: Muffin-Tin Orbitals and Electronic Structure* (Springer, Berlin, 2012).
- [31] I. Turek, V. Drchal, J. Kudrnovsky, M. Sob, and P. Weinberger, *Electronic Structure of Disordered Alloys, Surfaces and Interfaces* (Kluwer, Boston, 1997).
- [32] S. H. Vosko, L. Wilk, and M. Nusair, *Canadian Journal of Physics* **58**, 1200 (1980), <https://doi.org/10.1139/p80-159>.
- [33] P. A. Korzhavyi, A. V. Ruban, I. A. Abrikosov, and H. L. Skriver, *Phys. Rev. B* **51**, 5773 (1995).
- [34] B. Velický, S. Kirkpatrick, and H. Ehrenreich, *Phys. Rev.* **175**, 747 (1968).
- [35] F. H. Spedding, A. H. Daane, and K. W. Herrmann, *Acta Crystallographica* **9**, 559 (1956).